Two dimensional particle-in-cell simulations of the lunar wake

Paul C. Birch and Sandra C. Chapman

Citation: Physics of Plasmas (1994-present) **9**, 1785 (2002); doi: 10.1063/1.1467655
View online: http://dx.doi.org/10.1063/1.1467655
View Table of Contents: http://scitation.aip.org/content/aip/journal/pop/9/5?ver=pdfcov
Published by the AIP Publishing

Two dimensional particle-in-cell simulations of the lunar wake

Paul C. Birch and Sandra C. Chapman[a)]
Space & Astrophysics Group, Department of Physics, University of Warwick, Coventry, CV4 7AL, United Kingdom

(Received 31 October 2001; accepted 17 January 2002)

The solar wind plasma from the Sun interacts with the Moon, generating a wake structure behind it, since the Moon is to a good approximation an insulator, has no intrinsic magnetic field, and a very thin atmosphere. Following earlier one and one-half dimensional ($1\frac{1}{2}$D) simulations, $2\frac{1}{2}$D simulations have been studied for the first time. $2\frac{1}{2}$D simulations in the solar wind rest frame with an initial circular void reveal structures similar to those found in the earlier simulations, indicating that the $1\frac{1}{2}$D simulations are a good approximation to the physics. The infilling of the wake was found to be anisotropic, with the infilling occurring predominantly parallel to the magnetic field. The $2\frac{1}{2}$D simulations that are stationary with respect to the Moon, allow the effect of solar wind magnetic fields oblique to the solar wind flow to be studied, and these reveal additional assymetries. © *2002 American Institute of Physics.* [DOI: 10.1063/1.1467655]

I. INTRODUCTION

A wake structure is formed as the solar wind flows past the Moon. The Moon is to a good approximation an insulator, has no intrinsic magnetic field, and a very thin atmosphere. This results in the Moon being a sink for solar wind particles that collide with it. Directly behind the Moon, there will therefore be a void in which no solar wind particles are present. As the solar wind continues beyond the Moon, this wake is filled in.

Previously, high resolution one and one-half dimensional ($1\frac{1}{2}$D) particle-in-cell (PIC) simulations of the lunar wake have been performed[1] in good agreement with WIND spacecraft observations.[2] These simulations showed that the two-stream instability generated by the counterstreaming particle beams from either side of the wake is largely due to the presence of the counterstreaming electrons, rather than the counterstreaming ions. Peaked structures in the particle densities are associated with the propagating electron phase space holes, generated by the two-stream instability. An electron bump-on-tail instability was found just outside the wake, where electrons had passed through the wake and created an unstable distribution on the other side.

The $1\frac{1}{2}$D simulation employs a number of approximations and restricts the configuration of the interplanetary magnetic field (IMF) with respect to the solar wind flow. A major assumption of the $1\frac{1}{2}$D simulation is that the infilling of the lunar wake in the simulation box is not affected by the infilling perpendicular to the box. The $2\frac{1}{2}$D (two spatial; third component of E, B and velocities retained) simulations of the lunar wake in the solar wind rest frame, presented here, address this assumption.

In reality, the IMF can be directed in any direction, thus varying the exact nature of the interaction of solar wind with the Moon. The simulations run in the solar wind rest frame neglect flows parallel to the solar wind flow. The simulations stationary with respect to the Moon, presented here, allow these flows and oblique IMF angles to be simulated.

The simulations were performed using the same PIC code as the earlier $1\frac{1}{2}$D simulations.[1] The phase space resolution of the simulation scales as $\sim\sqrt{n}$, where n is the number of particles per cell. The $1\frac{1}{2}$D simulations[1] used $\sim$2500 particles per cell, however due to the higher number of grid cells required in simulations with two spatial dimensions, 256 particles per cell were employed, resulting in a significantly lower resolution. As a result, these simulations may not recover all the physics of interest. An ion to electron mass ratio of 20 has been chosen in order to evolve both ion and electron dynamics, as in the $1\frac{1}{2}$D simulations.[1]

II. $2\frac{1}{2}$D SIMULATIONS IN THE SOLAR WIND REST FRAME

Figure 1 shows the geometry of the simulation. The simulation box begins directly behind the Moon, perpendicular to the solar wind flow ($-X$ direction), with the IMF in the Y direction, analogous to the $1\frac{1}{2}$D simulations.[1] The simulation begins with a circular void in an otherwise Maxwellian distribution of ions and electrons which mimics the removal of solar wind particles by the Moon. As the simulation box moves with the solar wind, the simulation run time, t, can be equated to a distance behind the Moon, $v_{\mathrm{sw}}t$, provided the IMF and solar wind flow remain constant. The simulation run time is limited by the dimensions of the simulation box since all the boundaries are periodic. In these simulations a 256×256 grid cell simulation box has been used (grid cell $=$Debye length, λ_{D}) which equates to $\pm4R_L$ either side of an initial circular void of radius $32\lambda_{\mathrm{D}}$. A $1\frac{1}{2}$D simulation of length 256 grid cells, a void of 64 grid cells, and 256 particles per cell was run to verify that the same structures found in the higher resolution simulations[1] were repeated. All the structures were recoved in this test, except for the electrostatic waves generated by the electron bump-on-tail instability. The IMF strength has been scaled to 100 nT. This

a)Electronic mail: sandrac@astro.warwick.ac.uk

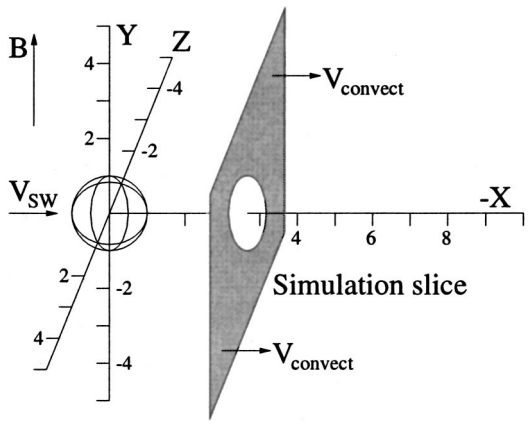

FIG. 1. Geometry of the simulation of the lunar wake in the solar wind rest frame.

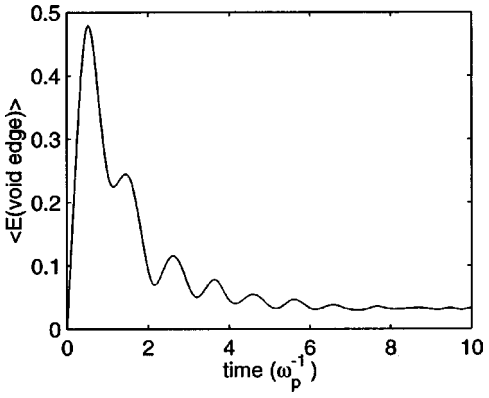

FIG. 3. Average electric field strength on the edge of the initial void against time, showing the ambipolar electric field oscillating at the plasma frequency.

is considerably higher than the ambient IMF strength, however, it is required for these simulations. With a 5 nT IMF, the radius of the simulation void ($R_L = 312$ m) is smaller than the simulation electron gyroradius ($r_{ge} = 1.4\times10^3$ m). This results in the void infilling equally from all directions. In reality, the void radius ($R_L = 1.74\times10^6$ m) is much larger than the electron gyroradius ($r_{ge} = 1.4\times10^3$ m), resulting in anisotropic infilling of the void. Choosing a value of 100 nT IMF yields a simulation electron gyroradius ($r_{ge} = 70$ m), which is 4.5 times smaller than the radius of the void ($R_L = 312$ m), thus recovering the scaling of the natural system. The IMF strength is chosen to ensure that the characteristic frequencies of the plasma will still be ordered as in the solar wind (i.e., $\omega_{pe} > \omega_{pi} > \Omega_e > \Omega_i$) otherwise different plasma physics will occur.

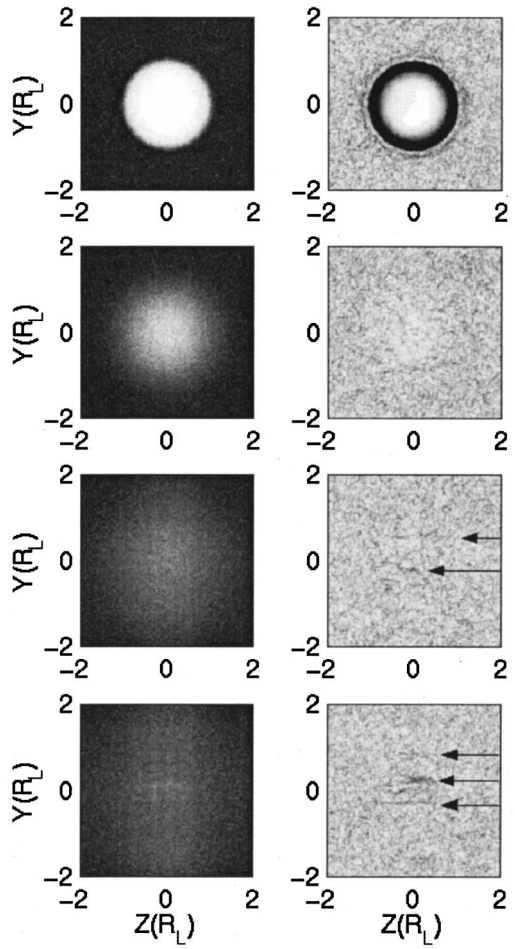

FIG. 2. Electron density and electric field magnitude at various times during the $2\frac{1}{2}$D simulation in the solar wind rest frame. The IMF is directed along *Y*. The series begins at $-X(R_L) = 1$ and then every $7R_L$. The arrows indicate the position of electron phase space tubes. Ambient plasma electron density is 5 cm^{-3}.

Results of the simulations

Figure 2 shows the evolution of electron density and electric field.[5] Initially, electrons begin to move into the void from all directions, however due to the presence of the IMF (and $R_L > r_{ge}$), the subsequent infilling is predominantly in the *Y* direction, resulting in the anisotropic infilling of the void. Differences between the electron and ion densities are indistinguishable at this level of resolution. Examination of the ion phase space $[Y(R_L)$ against $v_Y]$ shows the ions being accelerated into the void by the ambipolar electric field set up by the faster electrons, as in the $1\frac{1}{2}$D simulations.[1] This electric field is directed radially inwards and is shown in the first electric field plot in Fig. 2. This ambipolar electric field fluctuates in time. The electrons move in first, accelerating the ions in. The electrons then fluctuate about the ions. This can be shown by calculating the temporal variation of the average electric field strength on the edge of the initial void (Fig. 3). The ambipolar electric field oscillates at the plasma frequency and can be seen up to eight plasma periods. Ultimately, the infilling of the wake produces counterstreaming beams in the direction of the IMF. This generates a two-stream instability which saturates and produces electron phase space tubes, perpendicular to the IMF. These electron tubes are the 2D analog of the electron holes found in the $1\frac{1}{2}$D simulations[1] and propagate along the IMF. These tubes are evident in the electron density and electric field plots in Fig. 2 (indicated by arrows).

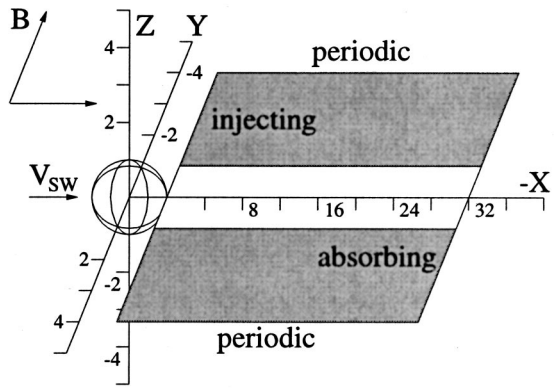

FIG. 4. Geometry of the simulation of the lunar wake, stationary with respect to the Moon. The IMF can be directed in any direction in the $X-Y$ plane.

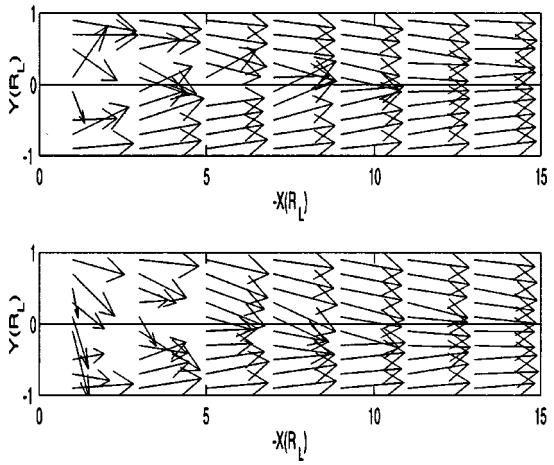

FIG. 5. Electron bulk velocities from the $2\frac{1}{2}$D simulations, stationary with respect to the Moon. The first plot is the simulation with the IMF at 90° to the solar wind flow while the second plot has the IMF at 60°.

III. $2\frac{1}{2}$D SIMULATIONS STATIONARY WITH RESPECT TO THE MOON

Figure 4 shows the geometry of the $2\frac{1}{2}$D simulations of the lunar wake, stationary with respect to the Moon. Since the plasma is given a drift velocity in the $-X$ direction, the simulation particles have to be injected at one boundary, apart from a section mimicking the removal of particles by the Moon, and absorbed at the opposite boundary. The other two boundaries are periodic, restricting the length (along X) of the simulation box. The physical size of the simulation box is 1024×300 grid cells with a void on the upstream boundary of 64 grid cells. The fastest particles will cross the wake and reach the periodic boundary in approximately the time it takes the plasma to drift the length of the simulation box (along X). The plasma parameters of the simulation are the same as those employed in the $1\frac{1}{2}$D simulations.[1] Two simulations have been run with this configuration, one with the IMF in the Y direction (i.e., 90° to the solar wind flow) and another with the IMF at an oblique angle (60° to the solar wind flow), highlighting some of the differences when the IMF is at an oblique angle. The 90° IMF simulation can be compared to the previous simulations, in the solar wind rest frame (both $1\frac{1}{2}$D and $2\frac{1}{2}$D).

Results of the simulations

The initial configuration of these simulations is unphysical. The simulations must go through a transient time while the first injected particles pass through the simulation and exit on the opposite boundary. This is approximately $29\omega_{pe}^{-1}$ and the results shown here are after this time. The infilling of the wake is very similar to all the previous simulations, up to about $-X=10R_L$, with the electrons entering the void first, setting up the ambipolar electric field and accelerating the ions toward the center. Beyond $10R_L$ behind the Moon, differences begin to occur. The expected two-stream instability does not appear to have grown. The 60° IMF simulation reveals a slight asymmetry due to the oblique angle between the IMF and the solar wind flow. The clearest asymmetry is found by considering the bulk velocities in the central wake regions. Figure 5 shows the electron bulk velocities for both the 90° and 60° IMF simulations. The erratic behavior of these velocity vectors comes predominantly from the fact that the error in these bulk velocity vector plots increases as the number of particles in the bin decreases (error $\propto 1/\sqrt{n}$). By comparing the electron bulk velocities at $-X=9R_L$ in both simulations, an asymmetry is apparent in the 60° IMF simulation. These vectors are more reliable since more particles were used to calculate them.

IV. TWO-STREAM INSTABILITY IN TWO SPATIAL DIMENSIONS

The absence of the two-stream instability in the $2\frac{1}{2}$D simulations, stationary with respect to the Moon, could be simply due to the size of the simulation box. By considering the phase spaces of both the electrons and the ions (not shown here) it can be seen that both species are in a counterstreaming beam distribution at the downstream absorbing edge of the simulation. Further, by considering the linear growth rate in a uniform plasma, the two-stream instability will grow given a longer simulation box. However, current computational resources prohibit such a simulation from being undertaken. In order to demonstrate that a two-stream instability would take place in a longer simulation box, further simulations have been performed. These simulations are not lunar wake simulations but evolve the full quasilinear and nonlinear two-stream instability in a nonuniform plasma. The simulation configuration is similar to Fig. 4. All the boundaries are now periodic and the dimensions of the simulations are just $64\lambda_D\times256\lambda_D$. The initial void is still $64\lambda_D$ across and all of the plasma parameters are the same as those used in the $2\frac{1}{2}$D simulations, stationary with respect to the Moon. Two simulations were performed, with the magnetic field at 90° and 60°, both for $50\omega_{pe}^{-1}$. When the two-stream instability is studied, simulations are usually set up with counterstreaming beams at $t=0$. These simulations, however, are effectively two colliding beams, not counterstreaming at $t=0$, but ultimately doing so once the beams interpenetrate.

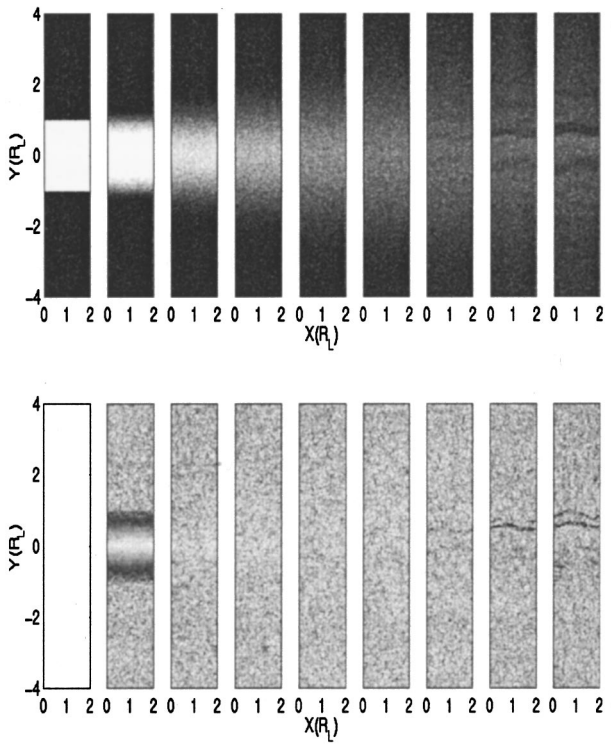

FIG. 6. Ion density and electric field magnitude of the $2\frac{1}{2}$D simulation of the generation of a two-stream instability from a plasma void. Ambient plasma ion density is 5 cm^{-3}. The first plot is at time $t=0$; the second plot is at $t=2.77\omega_{pe}^{-1}$; the time between each subsequent plot is $5.53\omega_{pe}^{-1}$.

Results of the simulations

The ion density from the 90° simulation, shown in the upper row of Fig. 6, shows the first signs of a two-stream instability after $30.7\omega_{pe}^{-1}$ (seventh plot). This, and other density enhancements, persist until the end of the simulation, growing in width. The plasma drift in the $2\frac{1}{2}$D simulations, stationary with respect to the Moon is 6.875×10^6 ms^{-1}, thus the two-stream instability should be detectable at about $34R_L$ downstream of the Moon, just off the downstream boundary of the simulation. The electric field of this simulation (lower row of Fig. 6) also shows the growth of the two-stream instability. The increases of the electric field across the simulation box, generated by the two-stream instability, appear to fluctuate. The plasma is forced to fluctuate with a wavelength that fits an integer number of times in the simulation box. It appears that the wavelength of these fluctuations are the width of the simulation box. The two-stream instability in the 60° simulation did not grow as quickly as in the 90° simulation and was not detectable in the electric field plot (not shown here), however there were slight enhancements in the ion density (not shown here). When studying trajectories of some electrons in the 90° simulation, it can be seen that they are trapped in the potentials created by the two-stream instability. The bounce periods of the particles are typically $6\omega_{pe}^{-1}$, thus the gyro-to-bounce frequency ratio is approximately 0.04. Muschietti *et al.*[3] showed that given a gyro-to-bounce frequency ratio greater than unity, the electron hole in two spatial dimensions will be stable and maintain its structure, while a frequency ratio less than unity results in unstable electron holes that oscillate along the length of the tube.[4]

V. CONCLUSIONS

Results from $2\frac{1}{2}$D simulations of the lunar wake have been presented here. Analogous to the $1\frac{1}{2}$D simulations,[1] the first simulation was run in the solar wind rest frame. Analysis of these simulations show the same structures as found with the $1\frac{1}{2}$D simulations.

In the $2\frac{1}{2}$D simulations in the solar wind rest frame we find:

(1) Electrons move in first, setting up the ambipolar electric field, pointing radially inwards.
(2) The ambipolar field oscillates at the plasma frequency.
(3) Particles traverse the void predominantly in the IMF direction, creating two-stream distributions.
(4) The infilling of the wake is anisotropic due to the IMF alignment.
(5) Electron phase space tubes are produced (analogous to the electron phase space holes found in $1\frac{1}{2}$D) and travel away from the wake along the IMF lines.

In $2\frac{1}{2}$D simulations (90° and 60° IMF), stationary with respect to the Moon we find that:

(1) An ambipolar electric field accelerates ions into void.
(2) Counterstreaming ion and electron beams are generated, persisting to the downstream edge.
(3) An asymmetry in the 60° IMF simulation revealed in electron bulk velocities.
(4) No two-stream instability evolves since the simulation boxes were too short in the direction of v_{sw}.

For the two-stream instability in two spatial dimensions we explored the full quasilinear and nonlinear evolution in a nonuniform plasma relevant to the lunar wake. We find:

(1) The two-stream instability occurred after approximately $30\omega_{pe}^{-1}$, in the 90° magnetic field case, equivalent to a downstream distance of $34R_L$ in the simulations stationary with respect to the Moon.
(2) Fluctuations of the electron tubes which were shown to be a result of the gyro-to-bounce ratio being less than unity.

The main result from these studies of $2\frac{1}{2}$D simulations of the lunar wake is that the results are very similar to the analogous $1\frac{1}{2}$D simulations. Therefore, the $1\frac{1}{2}$D simulation configuration is a good approximation to the physics, and give results that are a good comparison with the WIND flyby data.[2]

ACKNOWLEDGMENTS

This work has been funded by the Particle Physics and Astronomy Research Council (PPARC) and the Higher Education Funding Council of England (HEFCE).

[1]P. C. Birch and S. C. Chapman, Phys. Plasmas **8**, 4551 (2001).
[2]K. W. Ogilvie, J. T. Steinberg, R. J. Fitzenreiter, C. J. Owen, A. J. Lazarus, W. M. Farrell, and R. B. Torbert, Geophys. Res. Lett. **23**, 1255 (1996).
[3]L. Muschietti, R. E. Ergun, I. Roth, and C. W. Carlson, Geophys. Res. Lett. **26**, 1093 (1999).
[4]L. Muschietti, I. Roth, C. W. Carlson, and R. E. Ergun, Phys. Rev. Lett. **85**, 94 (2000).
[5]See EPAPS Document No. E-PHPAEN-9-040205 for color version of Fig. 2. This document may be retrieved via the EPAPS homepage (http://www.aip.org/pubservs/epaps.html) or from ftp.aip.org in the directory /epaps/. See the EPAPS homepage for more information.